# Geochemistry constraints of Mesozoic–Cenozoic calc-alkaline magmatism in the South Shetland arc, Antarctica

A. Machado[a,*], E.F. Lima[a], F. Chemale Jr.[a], D. Morata[b], O. Oteiza[b], D.P.M. Almeida[c], A.M.G. Figueiredo[d], F.M. Alexandre[a], J.L. Urrutia[b]

[a]*Institute of Geosciences, Federal University of Rio Grande do Sul, Isotope Geology Laboratory, Av. Bento Gonçalves, 9500, Campus do Vale, Agronomia, 91501-970 Porto Alegre, RS, Brazil*
[b]*Department of Geology, University of Chile, Casilla 13518, Correo 21, Santiago, Chile*
[c]*Department of Geology, Unisinos University, Av. Unisinos, 9500 São Leopoldo, RS, Brazil*
[d]*Institute of Energetic and Nuclear Research (IPEN) Nacional Commission of Nuclear Energy, Radiochemistry Division, University of São Paulo-USP, Post Box 11049, 01000 São Paulo, SP, Brazil*

**Abstract**

Geochemical data from basalts, basaltic andesites, and andesites of the Mesozoic–Cenozoic (143–44 Ma) from Livingston, Greenwich, Robert, King George, and Ardley Islands of the South Shetland archipelago, Antarctica, are presented. The rocks have variable $SiO_2$ of approximately 46–61 wt%, $Al_2O_3$ of 15–26 wt%, and total alkali ($K_2O + Na_2O$) of 2–6 wt%. Most samples have low Mg#, Cr, and Ni, which indicates that they have undergone significant fractional crystallization from mantle-derived melts. The presence of olivine cumulatic in the samples from Livingston and Robert Islands explains some high MgO, Ni, and Cr values, whereas low Rb, Zr, and Nb values could be related to undifferentiated magmas. N-MORB-normalized trace element patterns show that South Shetland Islands volcanic rocks have a geochemical pattern similar to that found for other island arcs, with enrichment in LILE relative to HFSE and in LREE relative to HREE. The geochemistry pattern and presence of calcic plagioclase, orthopyroxene, Mg-olivine, and titanomagnetite phenocrysts suggest a source related to the subduction process. The geochemical data also suggest magma evolution from the tholeiitic to the calc-alkaline series; some samples show a transitional pattern. Samples from the South Shetland archipelago show moderate LREE/HREE ratios relative to N-MORB and OIB, depletion in Nb relative to Yb, and high Th/Yb ratios. These patterns probably reflect magma derived from a lithospheric mantle source previously modified by fluids and sediments from a subduction zone.

*Keywords:* Antarctica; Calc-alkaline; Subduction zone; Tholeiitic

**Resumo**

Dados geoquímicos de basaltos, andesitos basálticos e andesitos mesozóicos–cenozóicos (143–44 Ma) das ilhas Livingston, Greenwich, Robert, King George e Ardley do Arquipélago Shetland do Sul, Antártica são discutidas neste artigo. As rochas tem conteúdos de $SiO_2$ variando de 46 a 61%, $Al_2O_3$ de 15 a 26% e álcalis ($K_2O + Na_2O$) de 2 a 6%. A maior parte das amostras tem conteúdos baixos de Mg#, Cr e Ni, indicando que sofreram significante cristalização fracionada de fusões derivadas do manto. A presença de fases cumuláticas nas amostras das ilhas Livingston e Robert explicaria os elevados valores de MgO, Ni, Cr, enquanto que baixos valores de Rb, Zr e Nb observados nas amostras destas ilhas poderiam estar relacionados a magmas não diferenciados. Os padrões de elementos-traço normalizados pelo N-MORB mostram que as rochas vulcânicas das Ilhas Shetland do Sul têm padrão geoquímico similar àqueles encontrados em outros arcos de ilhas com enriquecimento em LILE em relação aos HFSE e em ETRL em relação aos ETRP. O padrão geoquímico e a ocorrência de fenocristais de plagioclásio cálcico, ortopiroxênio, olivina magnesiana e titanomagnetita sugerem origem relacionada a processos de subducção. Dados geoquímicos obtidos para as amostras do arquipélago Shetland do Sul sugerem um magma evoluindo de toleítico para cálcico-alcalino,

* Corresponding author. Tel.: +55 51 33166398; fax: +55 51 33166340.
*E-mail address:* adrianemachado@yahoo.com.br (A. Machado).

observando-se em algumas amostras um padrão transicional. As amostras do arquipélago Shetland do Sul mostram em relação ao N-MORB e OIB, moderadas razões ETRL/ETRP, empobrecimento em Nb relativo a Yb e elevada razão Th/Yb Estes padrões refletem, provavelmente, magma derivado de uma fonte mantélica litosférica, que foi modificada por fluídos e sedimentos da zona de subducção.

*Keywords:* Antártica; Cálcico-alcalino; Toleítico; Zona de subducção

## 1. Introduction

New geochemistry data are presented for Mesozoic–Cenozoic volcanic and hypabissal rocks from Livingston, Robert, and Ardley Islands of the South Shetland arc, Antarctica. These rocks include basalts, basaltic andesites and andesites and are composed of subhedral–anhedral phenocrysts of plagioclase, augite, olivine, and Ti-magnetite. Glomeroporphyritic, porphyritic, pilotaxitic, intergranular, and intersertal textures are common. Geochemical data indicate an affinity between tholeiitic and calc-alkaline samples, though some samples present transitional behavior. The calc-alkaline rocks are richer in $Al_2O_3$, Rb, Ba, and Sr than the tholeiitic and are enriched in light rare-earth elements (LREE) relative to heavy rare-earth elements (HREE). The lower contents of Ni, Cr, and Co indicate that these rocks crystallized from evolved magmas. Some high Ni, Cr, Co, and MgO values may be explained by the presence of olivine as a cumulative phase in the samples from Robert and Livingston Islands.

The generation and subsequent evolution of magma in subduction zone settings is widely acknowledged as a multivariate process that involves possible inputs from the subducted oceanic lithosphere and sediments, as well as the asthenospheric and lithospheric portions of the mantle wedge above the subduction zone (Tatsumi and Eggins, 1995). Following melt generation, processes such as crystal fractionation, accumulation, and crustal assimilation during transit to the surface can obscure the true nature of the magma source. The effects of these processes on the composition of the erupted products thus must be removed before models of arc magma genesis can be tested, which makes it desirable to study rocks that have suffered minimal modification since separation from their source region. Magmas produced in subduction zone settings are complex geochemical mixtures, and understanding them is important because the growth and accretion of magmatic arcs represents a critical step in the growth and chemical evolution of the continental crust through time (Taylor and McLennan, 1985).

During the past 20 years, important advances have been made in identifying the principal factors involved in subduction zone magmatism (Arculus, 1994; Pearce and Peate, 1995). Melting takes place in the mantle wedge and is triggered by the introduction of hydrous fluids that have been released by the dehydration of the subducted slab. This material transfer from the slab to the wedge is responsible for the distinctive trace element features of arc magmas (Pearce, 1982). The extent to which elements are fractionated during the transfer process and as the fluid migrates through and equilibrates with the mantle wedge remains unclear (Pearce and Peate, 1995). The mechanism of slab-wedge transfer, probably a multistage process (Ellam and Hawkesworth, 1988), also is an issue. Differences in the incompatible element abundances of mantle wedge material before the addition of slab-derived components can be recognized both on a global scale and in individual arcs, but the origin of these variations is poorly understood (Arculus, 1994).

The South Shetland Islands represent a Jurassic–Quaternary, mature island arc founded on a sialic basement of schists and deformed sedimentary rocks (Smellie et al., 1984). Construction of the South Shetland Island arc began during the latest Jurassic or earliest Cretaceous in the southwestern part of the archipelago. The South Shetlands Islands lie approximately 950 km southeast of Cape Horn and 100 km northwest of the Antarctica Peninsula, from which they are separated by the Drake Passage and Bransfield Strait, respectively (Fig. 1). Geophysical evidence suggests that they are located on a small crustal plate, which may be defined by the oceanic trench to the west, along which subduction apparently has ceased (Barker and Griffiths, 1972).

This article presents the results of a geochemical investigation of samples collected from western Livingston Island (Byers Peninsula, Fig. 1(a)), southeastern Greenwich Island (Fort Point, Fig. 1(b)), western Robert Island (Coppermine Peninsula, Fig. 1(c)), southwestern King George Island (Fildes Peninsula, Fig. 1(d)), and northeastern Ardley Island (Fig. 1(d)) of the South Shetland archipelago.

## 2. Geochronology

All ages plotted in the maps were provided by previous literature (Grikurov et al., 1970; Pankhurst et al., 1979; Gracanin, 1983; Smellie et al., 1984; Hathway, 1997; Oteíza, 1999). The ages of the South Shetland samples vary from 143 to 44 Ma.

### *2.1. Byers Peninsula (Livingston Island)*

Previous stratigraphical work on the Byers Peninsula (Fig. 1(a)) has been summarized by Smellie et al. (1980) and Crame et al. (1993). Smellie et al. (1980) assign the Byers Peninsula succession to the Byers Formation, which they

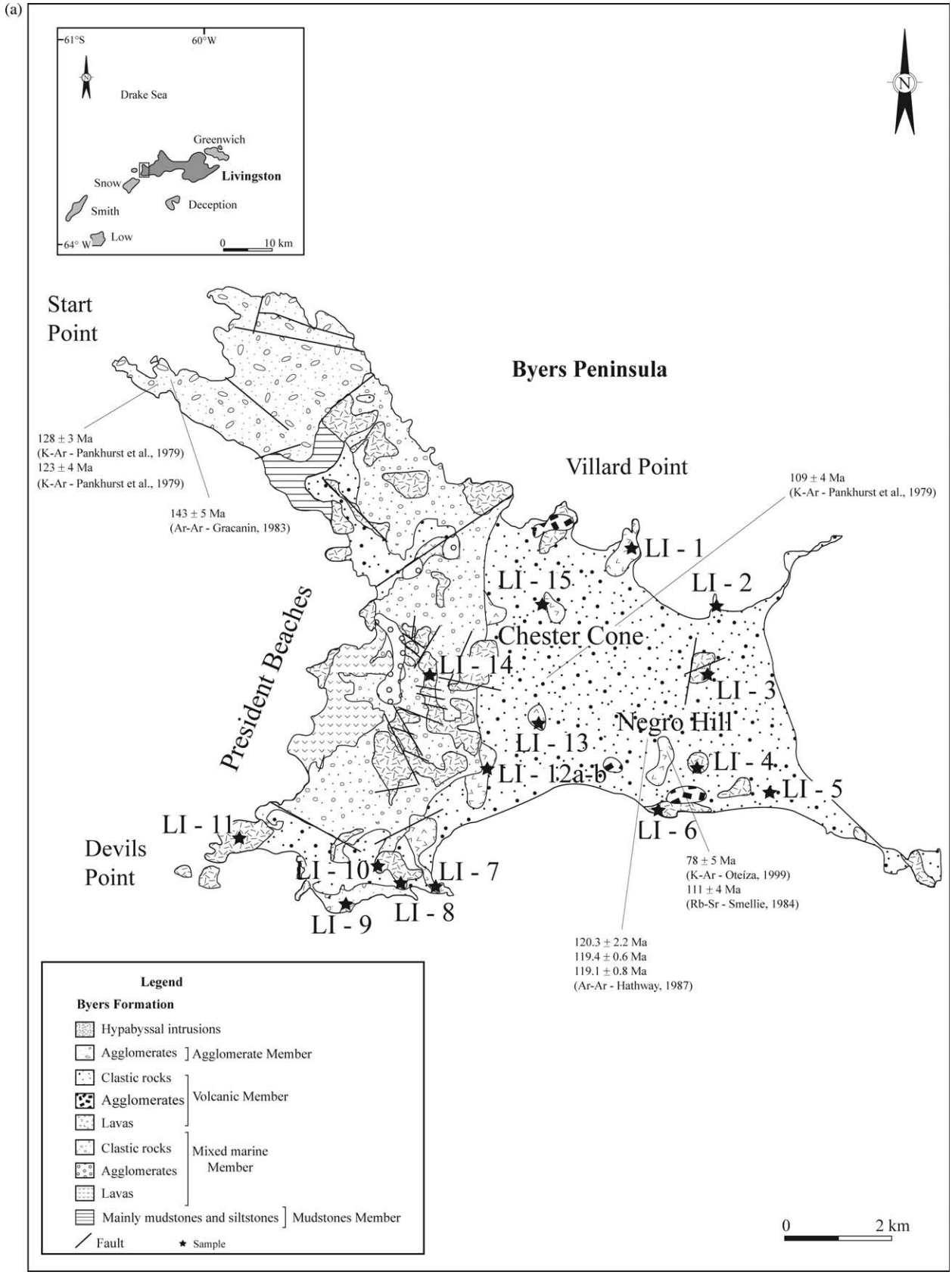


Fig. 1. Location map of the South Shetland Islands (modified from Machado, 1997). (a) Geological sketch map of Byers Peninsula (Livingston Island) with sample locations (modified from Smellie et al., 1984). (b) Location sketch map of Fort Point (Greenwich Island) with sample locations (modified from Azevedo, 1992). (c) Geological sketch map of Coppermine Peninsula (Robert Island) with sample locations (modified from Smellie et al., 1984). (d) Geological sketch map of Fildes Peninsula (King George Island) and Ardley Island with sample locations (modified from Machado, 1997).

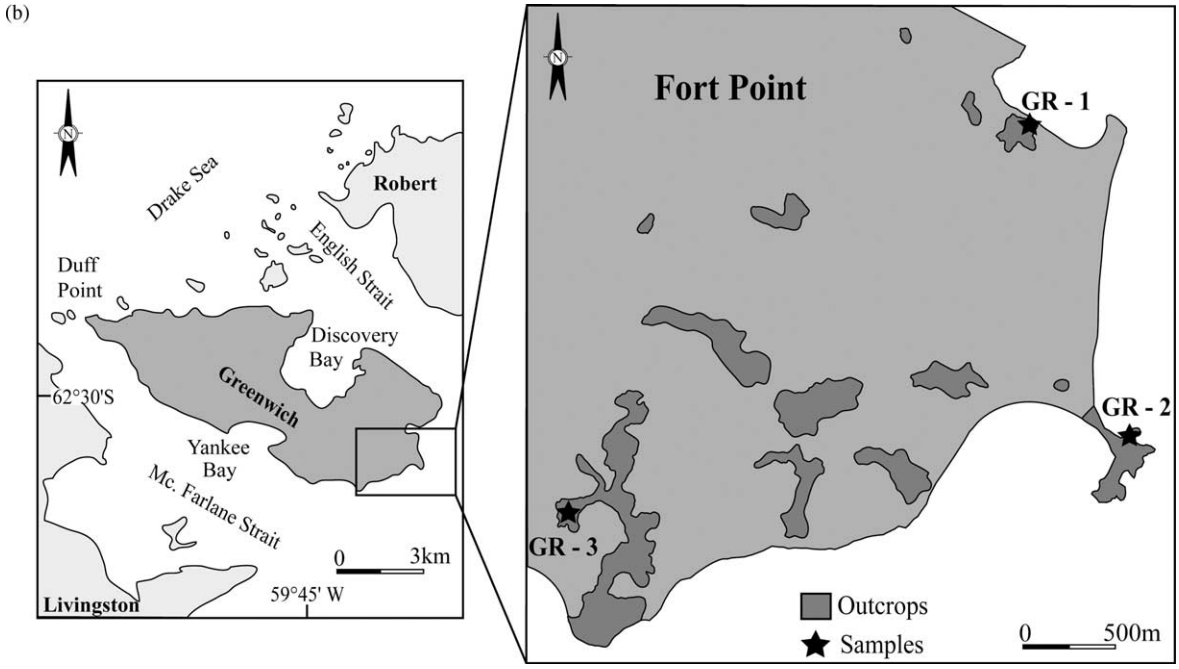


Fig. 1 (*continued*)

divide into four members: Mudstone, Mixed Marine, Agglomerate, and Volcanic. Crame et al. (1993) elevate the Byers Peninsula to group status, though assigned to the Byers Formation by Smellie et al. (1984), and divide the strata previously assigned to the Mudstone and Mixed Marine members into four formations: Anchorage, Devils Point, President Beaches, and Chester Cone. Hathway and Lomas (1998) revise and extend the lithostratigraphical scheme proposed for the western Byers Peninsula by Crame et al. (1993). Whereas Pankhurst et al. (1979) obtained whole-rock K–Ar ages of 128±3 and 123±4 Ma from minor intrusions in the volcanic breccias on the Start Point promontory, Gracanin (1983) obtained an admittedly discordant, whole-rock, Ar–Ar incremental heating spectrum on a basalt from the same area that indicated an age of 143±5 Ma. This finding suggests that the K–Ar ages may have been reset by Ar loss. Smellie et al. (1984) report a ten-point Rb–Sr isochron age of 111±4 Ma for ignimbrites from the lower part of the Cerro Negro Formation near Chester Cone. Pankhurst et al. (1979) obtain a K–Ar age of 109±4 Ma for a rhyolite lava southeast of Chester Cone. Silicic pyroclastic units close to the base of the Cerro Negro Formation have yielded Ar–Ar ages of 120.3±2.2 Ma for plagioclase from one sample and 119.4±0.6 and 119.1±0.8 Ma for biotite and plagioclase respectively from a second sample (Hathway, 1997). Oteíza (1999) obtains a K–Ar age of 78±5 Ma on a basaltic plug of Cerro Negro.

### 2.2. Fort point (Greenwich Island)

Volcanic rocks are represented by basalts, basaltic andesites, and andesites, whereas plutonic rocks are granites, tonalites, diorites, and gabbros. A K–Ar age of 105 Ma for a tonalite from the central part of the island was obtained by Grikurov et al. (1970). Smellie et al. (1984) indicate an age of 80±2 Ma for a basalt sill on Greenwich Island.

### 2.3. Coppermine Peninsula (Robert Island)

The Coppermine Formation is composed of olivine basalt lavas, rare basaltic andesites, polymict lapillistones, and agglomerates interbedded with basaltic andesite and andesite lavas. Conglomerates are restricted to the south-eastern Coppermine Peninsula. Multiple intrusions are common. K–Ar ages of 83–78±2 Ma (Smellie et al., 1984) for the lavas and sills from Coppermine Cove (Fig. 1(c)) are the first indication of the age of the rocks in the central part the South Shetland Islands. Smellie et al. (1984) obtain K–Ar ages of 60±1 Ma for a multiple sill at Fort William (Fig. 1(c)), which may have lost significant radiogenic Ar, especially because the latter sample is rather altered.

### 2.4. Fildes Peninsula (King George Island)

Smellie et al. (1984) obtain K–Ar ages of 58±5 and 47±2 Ma for volcanic rocks from the Fildes Peninsula. Plugs at Suffield Point (andesite) give a K–Ar age of 44±1 Ma. Stratigraphical studies identify four formations in the Fildes Peninsula Group: Clement Hill (basalts, basaltic andesites and andesites interbedded polymitic volcanic breccias), Fildes Strait (trachybasalts and porphyritic basalts associated with volcanic breccias), Schneider Bay

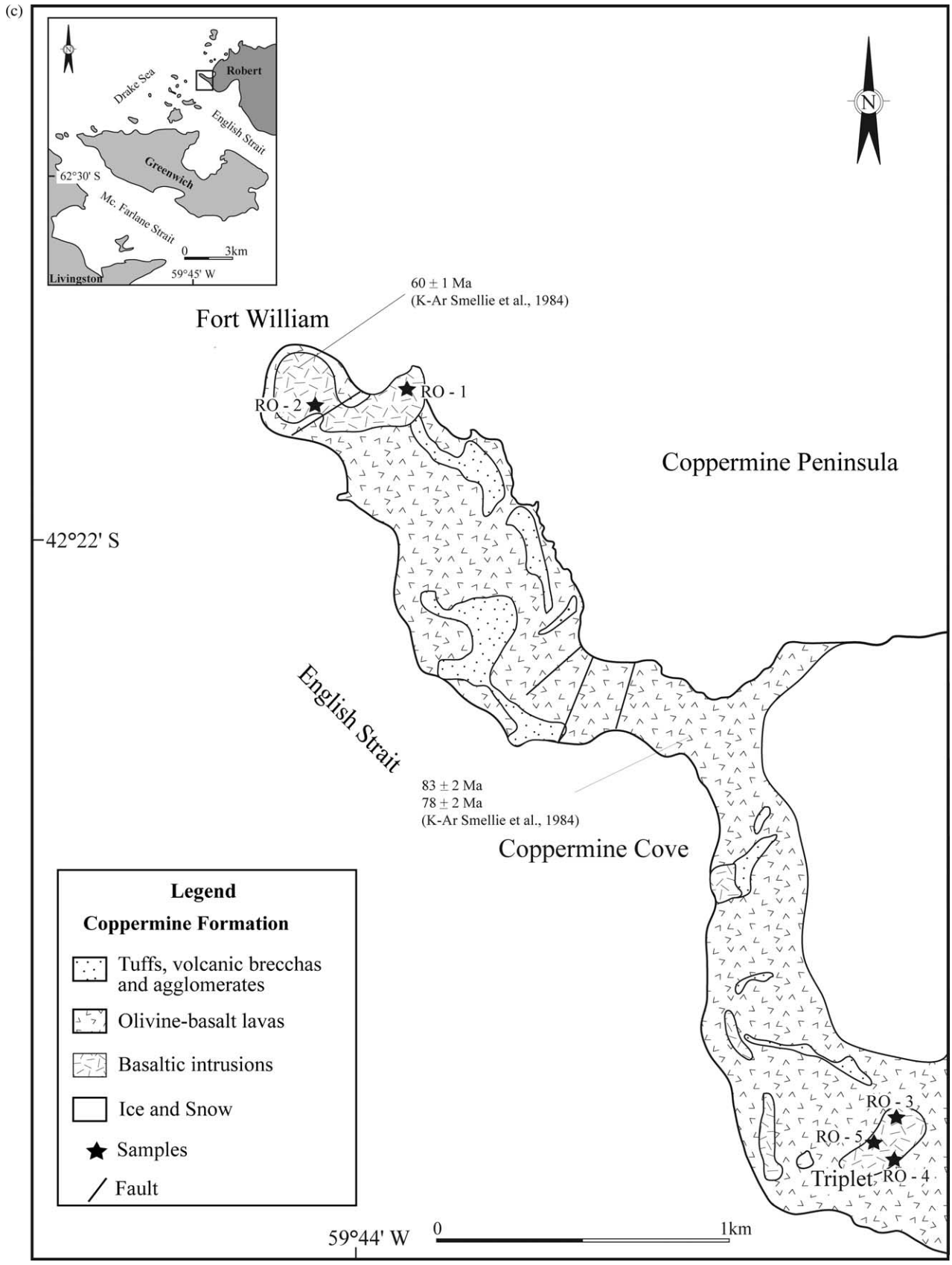


Fig. 1 (*continued*)

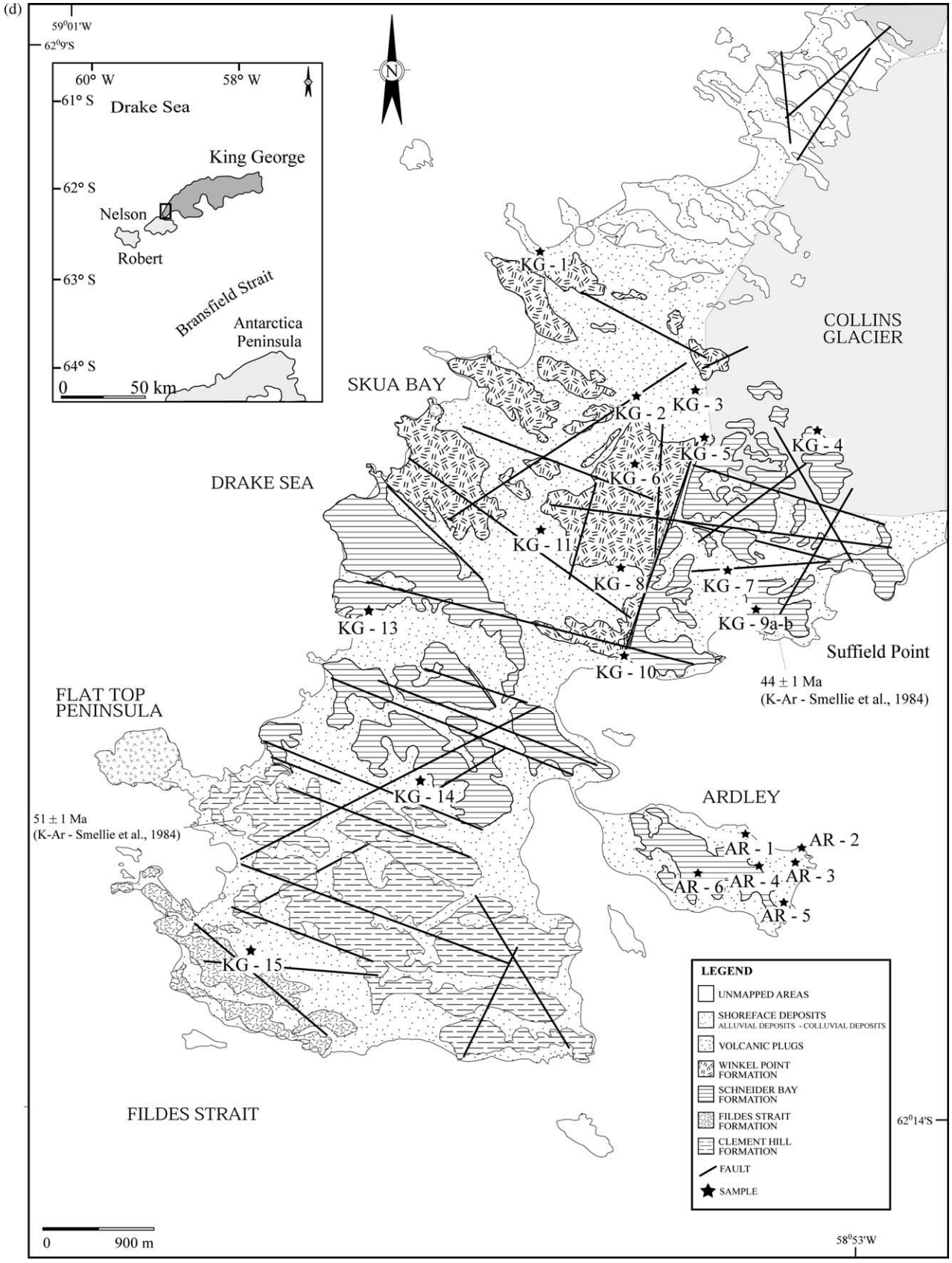


Fig. 1 (*continued*)

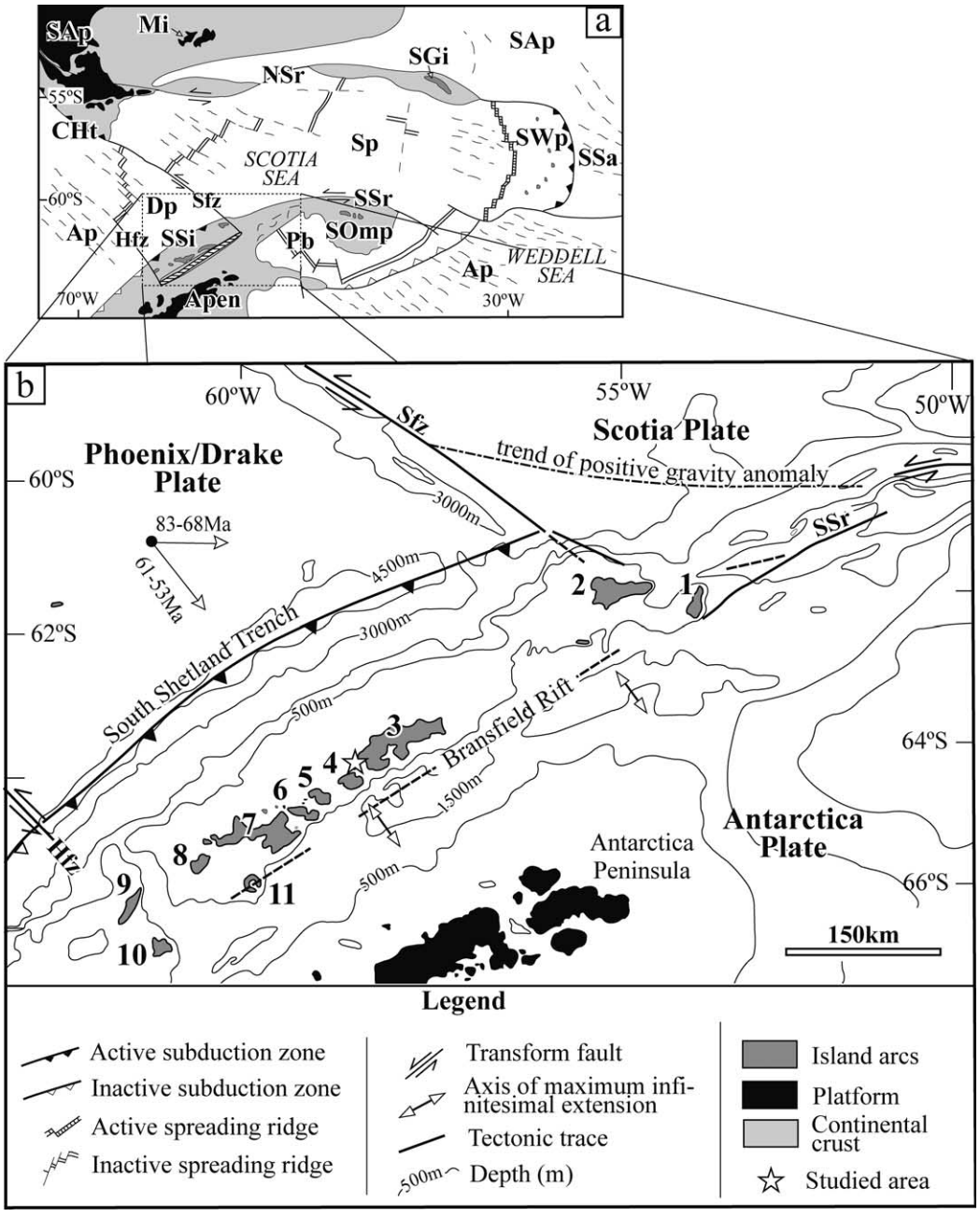


Fig. 2. Tectonostructural map of South Shetland archipelago and Antarctica Peninsula (González-Ferrán, 1985) and schematic section (AB) showing the relationship between arc magmatism and the fan-like rift system (arrows indicate the dominant strain field).

(porphyritic basalts, basaltic andesites, andesites, and dacites interbedded breccias), and Winkel Point (basalts and basaltic andesites interbedded volcanic breccias, agglomerates, conglomerates, and tuffs).

## 3. Geological setting

The tectonic context of the South America–Scotia–Antarctica plate junction has been related to a complex evolution from the Paleozoic–Mesozoic to the present. This evolution was accompanied by varied tectonic episodes that can be grouped into six major tectonic events from 250 to 20 Ma: (1) Paleozoic–Mesozoic Samfrau orogeny, (2) early processes of Gondwana fragmentation, (3) Gondwana breakup, (4) Phoenix plate subduction, (5) arc volcanism in the South Shetland Islands, and (6) extensional tectonism in the Antarctica Peninsula. It is widely accepted that the Antarctica Peninsula block had an important counterclockwise rotation in the Jurassic–Cretaceous, probably linked to the dispersion of the southern Gondwana (Pankhurst et al., 2000).

Table 1
Selected whole-rock analyses of volcanic rocks from South Shetland Islands

| Sample | Ardley Island | | | Greenwich Island | | | Robert Island | | | | |
|---|---|---|---|---|---|---|---|---|---|---|---|
| | AR-5 | AR-1 | AR-6 | GR-3 | GR-2 | GR-1 | RO-2 | RO-1 | RO-3 | RO-5 | RO-4 |
| $SiO_2$ | 51.73 | 53.78 | 55.72 | 47.47 | 53.95 | 55.99 | 48.09 | 49.13 | 49.21 | 49.31 | 49.40 |
| $TiO_2$ | 0.8 | 0.98 | 0.91 | 0.83 | 0.78 | 0.61 | 0.97 | 0.95 | 0.91 | 0.89 | 0.79 |
| $Al_2O_3$ | 18.15 | 17.14 | 17.05 | 25.74 | 18.87 | 17.4 | 16.93 | 17.64 | 18.2 | 17.50 | 18.3 |
| FeOt | 9.06 | 9.78 | 8.34 | 8.67 | 8.49 | 7.46 | 9.50 | 9.38 | 9.56 | 9.60 | 8.9 |
| MgO | 5.35 | 4.89 | 4.14 | 3.06 | 4.57 | 3.89 | 8.86 | 7.76 | 7.47 | 8.00 | 7.33 |
| MnO | 0.16 | 0.15 | 0.14 | 0.12 | 0.16 | 0.14 | 0.14 | 0.16 | 0.16 | 0.17 | 0.14 |
| CaO | 9.92 | 7.53 | 7.55 | 9.33 | 9.20 | 7.26 | 10.03 | 9.65 | 10.31 | 10.82 | 10.54 |
| $Na_2O$ | 2.91 | 3.03 | 3.13 | 3.23 | 2.95 | 3.67 | 2.66 | 3.17 | 2.58 | 2.51 | 2.64 |
| $K_2O$ | 0.52 | 0.77 | 0.92 | 0.45 | 0.20 | 1.05 | 0.58 | 0.68 | 0.28 | 0.21 | 0.3 |
| $P_2O5$ | 0.16 | 0.22 | 0.21 | 0.04 | 0.11 | 0.13 | 0.35 | 0.26 | 0.14 | 0.15 | 0.13 |
| LOI | 1.29 | 1.75 | 1.53 | 2.01 | 0.59 | 1.49 | 1.63 | 1.15 | 1.29 | 1.08 | 1.41 |
| Total | 100.06 | 100.06 | 99.66 | 100.95 | 99.87 | 98.57 | 99.73 | 99.90 | 100.09 | 100.24 | 99.88 |
| Mg# | 37.13 | 33.33 | 33.17 | 26.10 | 35.00 | 34.30 | 48.26 | 45.27 | 43.86 | 45.45 | 45.16 |
| Rb | 11 | 14 | 18 | 10 | 3 | 27 | 13 | 14 | 4 | 3 | 5.5 |
| Ba | 233 | 292 | 272 | 184 | 112 | 263 | 327 | 302 | 132 | 122 | 126 |
| Sr | 587 | 510 | 488 | 686.5 | 477.5 | 470 | 538 | 557 | 486 | 482 | 473 |
| Ni | 27 | 25 | 21 | 23 | 18 | 5 | 154 | 104 | 91 | 100 | 79 |
| Cr | 66 | 65 | 49 | 82 | 37 | 43 | 455 | 339 | 328 | 329 | 281 |
| Co | 46 | 28 | 35 | 23 | n.d. | n.d. | 41 | 38 | 37 | 47 | 34 |
| Nb | 3.9 | 3.8 | 3.8 | 1.24 | 1.1 | 3 | 2 | 1.7 | 1.1 | 0.7 | 1.6 |
| Zr | 59 | 119 | 109 | 44 | 55.5 | 95 | 76 | 88 | 47 | 41.5 | 45 |
| Y | 16 | 21 | 21 | 13 | 17.5 | 14.5 | 17.5 | 16 | 14 | 16 | 13 |
| Hf | n.d. | 3 | n.d. | 1 | 2 | 3 | 2 | 2.5 | 1 | n.d. | 1 |
| U | 1.5 | 0.6 | 0.3 | 0.2 | n.d. | n.d. | 1.5 | 2 | 0.2 | 1 | 0.3 |
| Th | 4.5 | 2 | 3.5 | 1 | 0.1 | 5 | 2 | 2 | 2 | 0.5 | 2 |
| Pb | 6 | 7 | 6 | < 5 | n.d. | n.d. | 5 | 4 | 4 | 2 | 1 |
| Ga | 19 | 20 | 19 | 23 | n.d. | n.d. | 18 | 19 | 18 | 18.5 | 17.5 |
| Cu | 129 | 152 | 173 | < 5 | n.d. | n.d. | 108 | 73 | 80 | 72 | 80 |
| Zn | 77 | 92 | 82 | 11 | n.d. | n.d. | 71 | 62 | 67 | 65 | 58 |
| Sc | 28.5 | 26 | 26 | 26 | 25 | 19 | 20 | 20 | 24 | 27.5 | 25.5 |
| V | 273 | 284 | 239 | 73 | 88 | 152 | 250 | 242 | 267 | 270 | 221 |
| Cs | n.d. | 3 | n.d. | 1 | n.d. | n.d. | n.d. | n.d. | n.d. | n.d. | n.d. |
| Ta | n.d. | n.d. | n.d. | 0.1 | 0.1 | 0.2 | n.d. | n.d. | n.d. | n.d. | n.d. |
| La | 8 | 13.1 | 11 | 5.22 | 5 | 12.25 | 13.9 | 11.9 | 5.1 | 3 | 4.9 |
| Ce | 24 | 29 | 36 | 12.17 | 11.65 | 24.71 | 30.4 | 25.8 | 11.9 | 15 | 11.0 |
| Pr | n.d. | n.d. | n.d. | 2 | 1 | 3 | n.d. | n.d. | n.d. | n.d. | n.d. |
| Nd | 13 | 18 | 17 | 8.72 | 8.17 | 12.57 | 18.3 | 15 | 8.28 | 9 | 6.24 |
| Sm | n.d. | 4 | n.d. | 2.19 | 2.35 | 2.84 | 4.46 | 3.87 | 2.17 | n.d. | 2.08 |
| Eu | 1.04 | 1.25 | n.d. | 0.94 | 0.89 | 0.88 | 1.30 | 1.22 | 0.83 | n.d. | 0.79 |
| Gd | n.d. | n.d. | n.d. | 2.05 | 2.73 | 2.86 | n.d. | n.d. | n.d. | n.d. | n.d. |
| Tb | n.d. | 0.61 | n.d. | 0.39 | 0.5 | 0.46 | 0.91 | 0.55 | 0.36 | n.d. | 0.38 |
| Dy | n.d. | n.d. | n.d. | 2.46 | 3.13 | 2.71 | n.d. | n.d. | n.d. | n.d. | n.d. |
| Ho | n.d. | n.d. | n.d. | 0.44 | 0.61 | 0.52 | n.d. | n.d. | n.d. | n.d. | n.d. |
| Er | n.d. | n.d. | n.d. | 1.26 | 1.93 | 1.61 | n.d. | n.d. | n.d. | n.d. | n.d. |
| Tm | n.d. | n.d. | n.d. | 0.16 | 0.28 | 0.22 | n.d. | n.d. | n.d. | n.d. | n.d. |

| | | | | | | | | | | | | | | | | |
|---|---|---|---|---|---|---|---|---|---|---|---|---|---|---|---|---|
| Yb | n.d. | 2.1 | n.d. | 1.47 | 1.89 | 1.61 | 1.59 | 1.70 | 1.40 | n.d. | 1.31 | | | | | |
| Lu | n.d. | 0.29 | n.d. | 0.2 | 0.31 | 0.28 | 0.21 | 0.21 | 0.2 | n.d. | 0.21 | | | | | |
| Sample | Livingston Island | | | | | | | | | | | | | | | |
| | LI-8 | LI-2 | LI-6 | LI-13 | LI-4 | LI-12b | LI-3 | LI-5 | LI-7 | LI-6 | LI-12a | LI-1 | LI-14 | LI-15 | LI-10 | LI-9 |
| $SiO_2$ | 48.41 | 48.4 | 49.5 | 49.6 | 50.4 | 50.54 | 50.7 | 53.07 | 53.6 | 53.88 | 54.00 | 55.46 | 56.73 | 57.96 | 60.90 | 60.98 |
| $TiO_2$ | 1.11 | 0.91 | 1.42 | 1.31 | 0.97 | 1.10 | 1.18 | 0.7 | 1.63 | 1.02 | 1.57 | 1.35 | 0.74 | 1.31 | 0.80 | 0.8 |
| $Al_2O_3$ | 20.51 | 18.29 | 15.9 | 17.3 | 16.0 | 17.03 | 15.9 | 16.93 | 15.9 | 19.63 | 16.0 | 15.27 | 17.42 | 15.07 | 16.77 | 16.69 |
| FeOt | 9.55 | 9.24 | 12.8 | 11.6 | 10.3 | 9.57 | 11.4 | 9.23 | 11.3 | 8.34 | 10.10 | 11.02 | 7.55 | 9.46 | 6.49 | 6.43 |
| MgO | 4.73 | 7.59 | 4.2 | 4.1 | 6.2 | 8.01 | 5.2 | 6.45 | 3.09 | 2.79 | 2.60 | 3.59 | 3.08 | 2.36 | 2.46 | 2.42 |
| MnO | 0.14 | 0.16 | 0.18 | 0.18 | 0.14 | 0.18 | 0.16 | 0.17 | 0.17 | 0.13 | 0.21 | 0.19 | 0.20 | 0.19 | 0.19 | 0.19 |
| CaO | 12.29 | 11.51 | 9.3 | 9.3 | 11.2 | 9.65 | 9.4 | 10.3 | 7.5 | 8.80 | 7.00 | 7.24 | 6.27 | 6.42 | 5.45 | 5.44 |
| $Na_2O$ | 2.47 | 2.37 | 3.6 | 3.9 | 3.1 | 2.88 | 3.7 | 2.66 | 4.1 | 3.97 | 4.40 | 3.99 | 4.15 | 3.72 | 4.31 | 4.24 |
| $K_2O$ | 0.28 | 0.42 | 0.62 | 0.33 | 0.26 | 0.19 | 0.81 | 0.5 | 1.35 | 0.96 | 0.68 | 1.05 | 1.03 | 0.66 | 1.04 | 1.03 |
| $P_2O5$ | 0.17 | 0.18 | 0.21 | 0.28 | 0.16 | 0.23 | 0.19 | 0.08 | 0.44 | 0.13 | 0.60 | 0.27 | 0.24 | 0.39 | 0.27 | 0.26 |
| LOI | 1.54 | 1.17 | 2.3 | 1.8 | 1.4 | 0.87 | 1 | 0.22 | 1.8 | 2.36 | 2.60 | 1.22 | 1.95 | 2.15 | 0.88 | 1.01 |
| Total | 101.20 | 100.25 | 100.3 | 100.5 | 99.3 | 100.25 | 99.7 | 100.34 | 101.2 | 102.01 | 101.6 | 100.65 | 99.36 | 99.71 | 99.55 | 99.51 |
| Mg# | 33.12 | 45.10 | 24.70 | 26.11 | 37.57 | 45.56 | 31.32 | 41.13 | 21.47 | 25.07 | 20.47 | 24.57 | 28.95 | 19.96 | 27.49 | 27.34 |
| Rb | n.d. | 5 | 8 | 5 | 2 | 3 | 10 | 7 | 23 | 22 | 14 | 21 | 17 | 25 | 22 | 18 |
| Ba | 71 | 295 | 75 | 126 | 77 | 87 | 109 | 91 | 245 | 176 | 308 | 180 | 145 | 329 | 227 | 204 |
| Sr | 525 | 574 | 461 | 476 | 341 | 369 | 317 | 284 | 362 | 369 | 490 | 260 | 377 | 438 | 329 | 302 |
| Ni | 8 | < 15 | < 15 | < 15 | 57 | 161 | 15 | 31 | < 15 | 6 | < 15 | 9 | <15 | < 15 | 15 | < 15 |
| Cr | 26 | 115 | 27 | 20 | 123 | 366 | 57 | 158 | 20 | 10 | 20 | 10 | 20 | 20 | 20 | 227 |
| Co | 29 | 49 | 60 | 22 | 52 | 62 | 43 | 42 | 23 | 22 | 40 | 20 | 16 | 34 | 29 | 24 |
| Nb | 6 | < 1 | < 1 | < 1 | 1 | 2.6 | 2 | 1 | 3 | 5 | 3 | 8 | 1 | 3 | 2 | 3 |
| Zr | 39 | 40 | 67 | 60 | 59 | 96 | 79 | 52 | 164 | 82 | 158 | 73 | 97 | 159 | 132 | 111 |
| Y | 13 | 10 | 27 | 20 | 17 | 23 | 21 | 17 | 35 | 25 | 41 | 29 | 21 | 36 | 26 | 24 |
| Hf | 1 | 1 | 2 | 2 | 2 | n.d. | 2 | 2 | 4 | 3 | 4 | 3 | 2.5 | 4.5 | 3.5 | 3 |
| U | n.d. | 0.2 | 0.2 | 0.2 | 0.1 | 0.7 | 0.3 | 0.3 | 0.7 | n.d. | 0.8 | n.d. | 0.5 | 1 | 0.6 | 0.6 |
| Th | 1 | 1 | 1 | 1 | 1 | 3 | 1 | 1.5 | 3 | 2.5 | 3 | 1.5 | 2 | 5 | 2 | 2 |
| Pb | n.d. | 5 | 5 | 5 | 5 | 4 | 5 | 5 | 5 | n.d. | 6 | n.d. | 5 | 7 | 5 | 5 |
| Ga | n.d. | 15 | 21 | 17 | 16 | 16 | 17 | 14 | 18 | n.d. | 20 | n.d. | 14 | 19 | 16 | 13 |
| Cu | 48 | 57 | 140 | 33 | 79 | 35 | 50 | 48 | 45 | 38 | 10 | 78 | 12 | 10 | 10 | 10 |
| Zn | 79 | 53 | 88 | 57 | 68 | 70 | 67 | 42 | 71 | 78 | 103 | 112 | 42 | 91 | 65 | 30 |
| Sc | 28 | 27 | 43 | 31 | 43 | 28 | 38 | 34 | 31 | 24 | 24 | 34 | 12.5 | 24 | 15 | 14 |
| V | 338 | 237 | 442 | 273 | 282 | 235 | 320 | 208 | 261 | 189 | 118 | 301 | 102 | 97 | 59 | 52 |
| Cs | n.d. | 0.5 | 0.5 | 1 | 0.5 | n.d. | 0.5 | 0.5 | 0.5 | n.d. | 7 | n.d. | 0.5 | 4.5 | 0.5 | 0.5 |
| Ta | n.d. | 0.1 | 0.1 | 0.1 | 0.2 | n.d. | 0.2 | 0.1 | 0.3 | n.d. | 0.3 | n.d. | 0.2 | 0.5 | 0.3 | 0.2 |
| La | 4 | 4.5 | 6.3 | 7.2 | 5.4 | 8 | 7.2 | 4.3 | 17.6 | 10 | 17.8 | 8 | 11.2 | 18.5 | 13.1 | 12.0 |
| Ce | 11 | 10.7 | 15.3 | 17.3 | 12.8 | 23 | 16.7 | 9.9 | 40.2 | 25 | 41.7 | 22 | 25.5 | 40.8 | 29.4 | 26.8 |
| Pr | n.d. | 1.5 | 2.24 | 2.47 | 1.73 | n.d. | 2.25 | 1.34 | 5.19 | n.d. | 5.76 | n.d. | 3.36 | 5.31 | 3.79 | 3.44 |
| Nd | 9 | 7.6 | 11.7 | 12.3 | 8.9 | 16 | 11.2 | 6.9 | 25.3 | 16 | 27.4 | 18 | 15.9 | 25.7 | 17.7 | 16.2 |
| Sm | 2.26 | 2.1 | 3.6 | 3.6 | 2.6 | n.d. | 3.2 | 1.9 | 6.4 | 3.7 | 7.1 | 4.05 | 3.7 | 6.1 | 4.4 | 4.0 |
| Eu | 0.79 | 0.87 | 1.43 | 1.28 | 0.98 | n.d. | 1.17 | 0.71 | 1.85 | 1.26 | 2.21 | 1.36 | 1.32 | 1.83 | 1.49 | 1.33 |
| Gd | 2.23 | 2.1 | 4.3 | 3.7 | 2.8 | n.d. | 3.5 | 2.2 | 6.1 | 3.98 | 7.5 | 4.23 | 3.9 | 6.6 | 4.6 | 4.0 |
| Tb | n.d. | 0.3 | 0.7 | 0.6 | 0.5 | n.d. | 0.6 | 0.4 | 1.0 | 0.58 | 1.1 | 1.01 | 0.6 | 1.0 | 0.7 | 0.6 |
| Dy | 2.35 | 1.8 | 4.6 | 3.5 | 3.0 | n.d. | 3.6 | 2.5 | 5.8 | 4.72 | 6.9 | 5.19 | 3.5 | 6.1 | 4.2 | 4.0 |
| Ho | 0.48 | 0.4 | 1.0 | 0.7 | 0.6 | n.d. | 0.7 | 0.5 | 1.2 | 0.96 | 1.4 | 1.09 | 0.7 | 1.3 | 0.9 | 0.8 |
| Er | 1.18 | 1.0 | 3.0 | 2 | 1.8 | n.d. | 2.3 | 1.7 | 3.7 | 2.65 | 4.2 | 2.98 | 2.2 | 3.6 | 2.8 | 2.4 |

(*continued on next page*)

Table 1 (*continued*)

| Sample | Livingston Island | | | | | | | | | | | | | | | |
|---|---|---|---|---|---|---|---|---|---|---|---|---|---|---|---|---|
| | LI-8 | LI-2 | LI-6 | LI-13 | LI-4 | LI-12b | LI-3 | LI-5 | LI-7 | LI-6 | LI-12a | LI-1 | LI-14 | LI-15 | LI-10 | LI-9 |
| Tm | n.d. | 0.14 | 0.45 | 0.31 | 0.27 | n.d. | 0.34 | 0.25 | 0.54 | n.d. | 0.61 | n.d. | 0.33 | 0.55 | 0.43 | 0.38 |
| Yb | 1.21 | 0.9 | 2.8 | 2.0 | 1.7 | n.d. | 2.1 | 1.7 | 3.3 | 2.7 | 3.7 | 2.99 | 2.3 | 3.4 | 2.7 | 2.5 |
| Lu | 0.19 | 0.13 | 0.44 | 0.29 | 0.26 | n.d. | 0.34 | 0.25 | 0.52 | 0.4 | 0.6 | 0.46 | 0.35 | 0.55 | 0.45 | 0.4 |
| Sample | King George Island | | | | | | | | | | | | | | | |
| | KG-10 | KG-12 | KG-1 | KG-11 | KG-15 | KG-6 | KG-5 | KG-14 | KG-7 | KG-13 | KG-2 | KG-9b | KG-9a | KG-8 | KG-3 | KG-4 |
| $SiO_2$ | 46.91 | 49.8 | 50.19 | 50.34 | 50.5 | 50.98 | 52.03 | 52.14 | 52.3 | 52.64 | 53.22 | 54.16 | 54.89 | 55.39 | 57.16 | 60.92 |
| $TiO_2$ | 0.62 | 0.75 | 0.84 | 0.45 | 0.84 | 0.78 | 1.06 | 0.85 | 0.84 | 0.71 | 0.88 | 0.78 | 0.78 | 0.7 | 0.96 | 0.97 |
| $Al_2O_3$ | 23.15 | 18.68 | 19.89 | 20.56 | 19.7 | 19.05 | 18.73 | 17.96 | 18.85 | 20.64 | 17.18 | 19.08 | 18.57 | 19.19 | 17.34 | 16.81 |
| FeOt | 7.83 | 9.04 | 9.64 | 7.59 | 10.28 | 9.06 | 9.2 | 10.05 | 9.03 | 7.96 | 8.22 | 8.03 | 7.99 | 8.81 | 8.03 | 6.58 |
| MgO | 4.61 | 5.85 | 4.31 | 6.15 | 4.33 | 5.08 | 3.91 | 3.73 | 4.75 | 4.25 | 4.68 | 3.7 | 3.72 | 2.9 | 3.13 | 2.85 |
| MnO | 0.16 | 0.17 | 0.18 | 0.12 | 0.17 | 0.15 | 0.2 | 0.18 | 0.11 | 0.14 | 0.14 | 0.2 | 0.15 | 0.16 | 0.29 | 0.16 |
| CaO | 11.00 | 11.7 | 9.97 | 10.90 | 9.78 | 10.73 | 8.1 | 7.79 | 7.76 | 10.39 | 8.35 | 8.48 | 8.49 | 7.34 | 7.15 | 5.25 |
| $Na_2O$ | 2.66 | 2.46 | 3.31 | 2.16 | 3.14 | 2.9 | 3.58 | 3.58 | 3.89 | 1.84 | 3.18 | 3.14 | 3.51 | 4.06 | 4.3 | 3.46 |
| $K_2O$ | 0.51 | 0.58 | 0.57 | 0.79 | 0.48 | 0.3 | 1.34 | 0.67 | 0.92 | 0.4 | 1.03 | 0.91 | 0.8 | 0.92 | 0.81 | 1.02 |
| $P_2O5$ | 0.09 | 0.22 | 0.13 | 0.09 | 0.13 | 0.16 | 0.26 | 0.15 | 0.19 | 0.12 | 0.14 | 0.21 | 0.2 | 0.22 | 0.27 | 0.31 |
| LOI | 2.54 | 0.88 | 1.01 | 1.78 | 0.67 | 0.8 | 1.26 | 2.03 | 0.95 | 0.11 | 2.62 | 1.29 | 1.1 | 0.36 | 0.47 | 0.81 |
| Total | 100.08 | 100.13 | 100.04 | 100.93 | 100.02 | 99.99 | 99.69 | 99.13 | 99.61 | 99.53 | 99.64 | 100 | 100.2 | 100.06 | 99.92 | 99.47 |
| Mg# | 37.05 | 39.30 | 30.90 | 44.76 | 29.64 | 35.93 | 29.82 | 27.07 | 34.50 | 34.80 | 36.28 | 31.54 | 31.77 | 24.80 | 28.05 | 30.22 |
| Rb | 6 | 6.5 | 5 | 11 | 4 | 8 | 28 | 11 | 13 | 7 | 18 | 23 | 24 | 17 | 42 | 22.5 |
| Ba | 263 | 284 | 149 | 155 | 218 | 171 | 354 | 174 | 295 | 151 | 204 | 280 | 292 | 242 | 349 | 464 |
| Sr | 672 | 665 | 575 | 608.5 | 613.5 | 601 | 487 | 514 | 568 | 573 | 467 | 593 | 569.5 | 615 | 472 | 487 |
| Ni | 16 | 28 | 88 | 6 | < 5 | 17 | 22 | < 5 | 29 | 9 | 56 | 21 | 22 | 3 | 12 | n.d. |
| Cr | 13 | 50 | 59 | 105 | 43 | 34 | 39 | 68 | 73 | n.d. | 123 | 50 | 50 | n.d. | 15 | n.d. |
| Co | 35 | 42 | 31 | 33 | 28.5 | 43 | 29 | 27 | 34 | 27.5 | 28 | 31 | 44 | 31 | 40 | 14.5 |
| Nb | < 0.4 | 1.8 | 0.90 | 0.93 | 1.57 | 1.1 | 5.7 | 1.54 | 3.5 | 0.6 | 4 | 4.5 | 3.4 | 1.1 | 5.4 | 6 |
| Zr | 29 | 63 | 44 | 54 | 46 | 57 | 127 | 64 | 101 | 92 | 97 | 100 | 88.5 | 97.7 | 122 | 166 |
| Y | 10.5 | 16 | 12 | 10 | 12 | 15 | 25.5 | 16 | 18 | n.d. | 1 | 21 | 17 | 19 | 25 | n.d. |
| Hf | n.d. | n.d. | 1.5 | 1 | 1 | n.d. | n.d. | 2 | n.d. | 2 | 2.5 | n.d. | n.d. | n.d. | n.d. | 3 |
| U | 0.6 | 1 | 0.3 | 0.6 | 0.4 | 0.8 | 2 | 0.4 | 1 | n.d. | 0.8 | 1 | 0.3 | 1.5 | 1 | n.d. |
| Th | 3 | 5.5 | 1 | 3 | 1 | 3.5 | 5 | 1 | 4 | 2 | 3 | 4.5 | 4.5 | 3.5 | 5.5 | 3 |
| Pb | 3 | 3 | 5 | 5 | 5 | 2 | 8 | 5 | 7 | n.d. | 5 | 9 | 6 | 4 | 6 | n.d. |
| Ga | 19 | 18 | 24 | 20 | 25 | 19 | 22.5 | 24 | 22 | n.d. | 23 | 21.5 | 19 | 21 | 19 | n.d. |
| Cu | 108 | 118 | 113 | 64 | 150 | 137 | 143 | 159 | 137 | n.d. | 64 | 101 | 104 | 81 | 94 | n.d. |
| Zn | 55 | 72 | 34 | 31 | 21 | 77 | 87 | 59 | 62 | n.d. | 12 | 95 | 74 | 86 | 84 | n.d. |
| Sc | 27 | 29 | 31 | 26 | 31 | 29 | 35.5 | 27 | 32 | 27 | 28 | 22 | 23.5 | 16 | 25 | 24 |
| V | 273 | 290 | 319 | 167 | 311 | 292 | 311 | 263 | 267 | 246 | 218 | 211 | 221 | 171 | 221 | 197.6 |
| Cs | n.d. | n.d. | 0.20 | 0.3 | 0.10 | n.d. | n.d. | 0.2 | n.d. | n.d. | 0.50 | n.d. | n.d. | n.d. | n.d. | n.d. |
| Ta | n.d. | n.d. | 0.1 | 0.1 | 0.1 | n.d. | n.d. | 0.1 | n.d. | n.d. | 0.3 | n.d. | n.d. | n.d. | n.d. | n.d. |
| La | 4 | 16 | 6.45 | 6.24 | 7.03 | 8 | 17 | 7.69 | 12 | 7.2 | 10.24 | 14 | 10 | 12 | 15 | 16.04 |
| Ce | 12 | 42 | 14.0 | 13.88 | 15.12 | 25 | 41 | 16.38 | 28 | 16.60 | 21.98 | 35 | 29 | 30 | 37 | 32.82 |
| Pr | n.d. | n.d. | 1.820 | 2 | 2 | n.d. | n.d. | 2 | n.d. | n.d. | 3 | n.d. | n.d. | n.d. | n.d. | n.d. |
| Nd | 9 | 24 | 9.68 | 8.76 | 10.07 | 12 | 24 | 11.67 | 21 | 13 | 13.98 | 17 | 18 | 17 | 21 | 21 |
| Sm | n.d. | n.d. | 2.76 | 2.15 | 2.70 | n.d. | n.d. | 2.96 | n.d. | 2.6 | 3.42 | n.d. | n.d. | n.d. | n.d. | 4.8 |
| Eu | n.d. | n.d. | 0.92 | 0.63 | 0.99 | n.d. | n.d. | 1 | n.d. | 1.02 | 1 | n.d. | n.d. | n.d. | n.d. | 1.6 |
| Gd | n.d. | n.d. | 2.36 | 1.57 | 2.24 | n.d. | n.d. | 2.64 | n.d. | n.d. | 2.94 | n.d. | n.d. | n.d. | n.d. | n.d. |

| | | | | | | | | | | | | | | | | | | | | |
|---|---|---|---|---|---|---|---|---|---|---|---|---|---|---|---|---|---|---|---|---|
| Tb | n.d. | n.d. | 0.39 | 0.27 | 0.41 | n.d. | n.d. | 0.46 | n.d. | n.d. | 0.50 | n.d. | n.d. | n.d. | n.d. | n.d. | n.d. | n.d. | n.d. | 0.59 |
| Dy | n.d. | n.d. | 2.34 | 1.86 | 2.5 | n.d. | n.d. | 3.09 | n.d. | n.d. | 2.8 | n.d. | n.d. | n.d. | n.d. | n.d. | n.d. | n.d. | n.d. | n.d. |
| Ho | n.d. | n.d. | 0.45 | 0.30 | 0.49 | n.d. | n.d. | 0.59 | n.d. | n.d. | 0.55 | n.d. | n.d. | n.d. | n.d. | n.d. | n.d. | n.d. | n.d. | n.d. |
| Er | n.d. | n.d. | 1.27 | 0.93 | 1.24 | n.d. | n.d. | 1.64 | n.d. | n.d. | 1.5 | n.d. | n.d. | n.d. | n.d. | n.d. | n.d. | n.d. | n.d. | n.d. |
| Tm | n.d. | n.d. | 0.158 | 0.142 | 0.186 | n.d. | n.d. | 0.233 | n.d. | n.d. | 0.211 | n.d. | n.d. | n.d. | n.d. | n.d. | n.d. | n.d. | n.d. | n.d. |
| Yb | n.d. | n.d. | 1.08 | 1.06 | 1.24 | n.d. | n.d. | 1.59 | n.d. | 1.2 | 1.41 | n.d. | n.d. | n.d. | n.d. | n.d. | n.d. | n.d. | n.d. | 2.12 |
| Lu | n.d. | n.d. | 0.20 | 0.16 | 0.210 | n.d. | n.d. | 0.27 | n.d. | 0.19 | 0.27 | n.d. | n.d. | n.d. | n.d. | n.d. | n.d. | n.d. | n.d. | 0.37 |

n.d., not determined.

The collision of a spreading center at the Antarctica Peninsula trench caused the migration of magmatism along the Antarctica Peninsula from Palmer and Graham to the South Shetland arc, where four phases of island arc volcanism have been identified: 130–110, 90–70, 60–40, and 30–20 Ma (Birkenmajer et al., 1986).

The islands of the central portion of the South Shetland archipelago provide the records of the last Phoenix–Antarctic interaction, including Cretaceous–Tertiary plutonovolcanosedimentary sequences of calc-alkaline affinity (Smellie et al., 1984) and Quaternary stratovolcanoes of alkalic basalts (Hole and LeMasurier, 1994) along the axis of the Bransfield rift (Fig. 2). In these islands, the dominant tectonic regime is extensional and restricted to volcanic arc areas where Tertiary volcanosedimentary activity predominates in association with normal faults, strike-slip faults, and intense tensional fracturing (Hamilton, 1995; Moore and Twiss, 1995).

## 4. Analytical techniques

Whole-rock samples were analyzed for major and trace elements by X-ray fluorescence (XRF) at the Department of Geology and Geophysics, University of Adelaide. All samples were crushed in a tungsten carbide jaw crusher after the weathered rims were removed. Loss on ignition (LOI) was determined from approximately 4 g of predried sample by heating to 960 °C overnight. Major elements were determined on fused glass discs using a lithium meta-/tetraborate flux sample (flux ratio = 1/4) with a Philips PW 1480 100 kV spectrometer. Trace elements were analyzed on pressed powder pellets. Reproducibility is generally better than $\pm 1\%$ for major elements and approximately $\pm 5\%$ for trace elements. The accuracy of the measurements, as determined by analyses of international standards, is better than $\pm 5\%$ for all elements except Ba, Ni, Zn, Cu, and Cr, for which accuracy is better than $\pm 10\%$. Some trace elements analyses were performed at the Institute of Energetic and Nuclear Research (IPEN), São Paulo, Brazil, by ICP-MS according to the methods described by Figueiredo and Marques (1989). Rare-earth elements (REE) were determined by ICP-MS at ACTLABS in Canada.

## 5. Petrography

The volcanic and hypabyssal rocks from Livingston, Greenwich, Robert, King George, and Ardley Islands show porphyritic, glomeroporphyritic, intergranular, pilotaxitic, and intersertal textures. Glomeroporphyritic textures involve phenocrysts of plagioclase, augite, olivine, and Ti-magnetite or only plagioclase, which suggests accumulation process.

The plagioclase phase exhibits a wide compositional range in basic and intermediate samples ($An_{42–85}$), with

a maximum anorthite (An) content of approximately 96 mol%. Pyroxenes from basic and intermediate rocks show similar chemistry compositions ($Wo_{23–48}$, $En_{40–58}$, $Fs_{9–21}$). Bronzite phenocrysts are present in one basaltic andesite from King George Island. Phenocrysts and microphenocrysts of olivine are generally altered to bowlingite or iddingsite and show compositions from $Fo_{71}$ to $Fo_{82}$. Almost all samples from Robert Island present well-preserved olivine phenocrysts.

The groundmass is composed of lath-shaped plagioclase microlites and augite, as well as rare pigeonite, olivine, Ti-magnetite, and volcanic glass.

## 6. Geochemistry

### 6.1. Major oxides

Whole-rock geochemistry data are listed in Table 1. Weathered rocks and those with high LOI were excluded. All samples analyzed from the South Shetland Islands are subalkaline, and the majority plot in the basalt and basaltic andesite field with a few samples in the andesite field according to LeMaitre's (2002) petrochemical classification. The majority of samples plot in the medium-K field, though a few plot in the low-K field (Fig. 3) according to the designation developed by Peccerillo and Taylor (1976).

MgO (2–9 wt%) was chosen as the differentiation index because it displays the best correlations with other major oxides. Diagrams of major elements versus MgO appear in Fig. 4. High MgO values (>7 wt%) are observed in two samples from Livingston Island (LI-2 and LI-12b) and in all samples from Robert Island (RO-1-RO-5), which probably reflect the accumulation of mafic phases such as olivine and clinopyroxene.

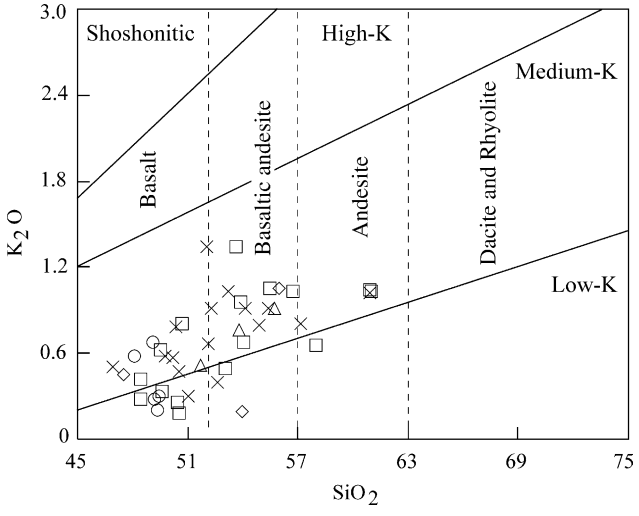


Fig. 3. Diagram of $SiO_2$ versus $K_2O$ with fields for low-K to shoshonitic rocks (LeMaitre, 2002). Symbols: □ = Livingston Island, ◇ = Greenwich Island, ○ = Robert Island, × = King George Island, and △ = Ardley Island.

For samples of all islands with MgO <7 wt%, the $TiO_2$ content increases with decreasing MgO to approximately 3 wt% MgO. This trend may reflect significant Ti-magnetite fractionation.

The samples have moderate to very high aluminum (15–26 wt% $Al_2O_3$) with considerable scatter, probably as a result of variations in the plagioclase abundance. CaO decreases with decreasing MgO for almost all samples, reflecting the strong clinopyroxene and plagioclase fractionation.

FeOt decreases with increased differentiation; this pattern may be related to olivine and clinopyroxene fractionation. The olivine phase is important in the rocks from Robert Island that show high values of MgO and FeOt. $Na_2O$ and $K_2O$ show non-linear negative correlations with MgO, common in a magmatic system that involves fractionation of calcic plagioclase and clinopyroxene.

$P_2O_5$ is incompatible in the majority of samples except those from Robert Island. This feature may be related to the presence of apatite in the mafic cumulates.

### 6.2. Trace elements

Variations in the trace element concentrations with MgO are shown in Fig. 5. Rb shows similar patterns to $K_2O$, and Sr and Ba contents show as much scatter as $Al_2O_3$. The elements have non-linear negative correlations with MgO, which suggests the influence of plagioclase fractionation (Vukadinovic, 1993). The rocks from Livingston Island that have lower Sr and Ba values also have lower aluminum contents. Zr and Nb contents show incompatible behavior with decreasing MgO, as does Y in samples other than those from Robert Island. This trend may be related to the presence of apatite in mafic cumulates.

Almost all samples have Th contents between 1 and 5 ppm. These values are typical of medium-K volcanic suites in an orogenic environment, according to Gill (1981).

Ni, Cr, Sc, and V contents exhibit a decline with decreasing MgO. This compatible behavior reflects the influence of olivine and clinopyroxene removal during suite evolution. The presence of cumulatic phases in the samples from Robert and Livingston Islands may explain some high values of MgO, Ni, and Cr. However, the low values of Rb, Zr, and Nb observed in samples from Robert Island are similar to those of the higher MgO, relatively undifferentiated samples.

All analyzed rocks have chondrite-normalized patterns enriched in LREE relative to HREE, which is typical of calc-alkaline suites. Some samples from Livingston, Greenwich, Robert, and King George Islands show weak positive Eu anomalies (Fig. 6), a possible reflection of plagioclase accumulation during magma evolution. Other samples from Livingston, Robert, and Ardley Islands show negative Eu anomalies (Fig. 6), probably associated with plagioclase fractionation.

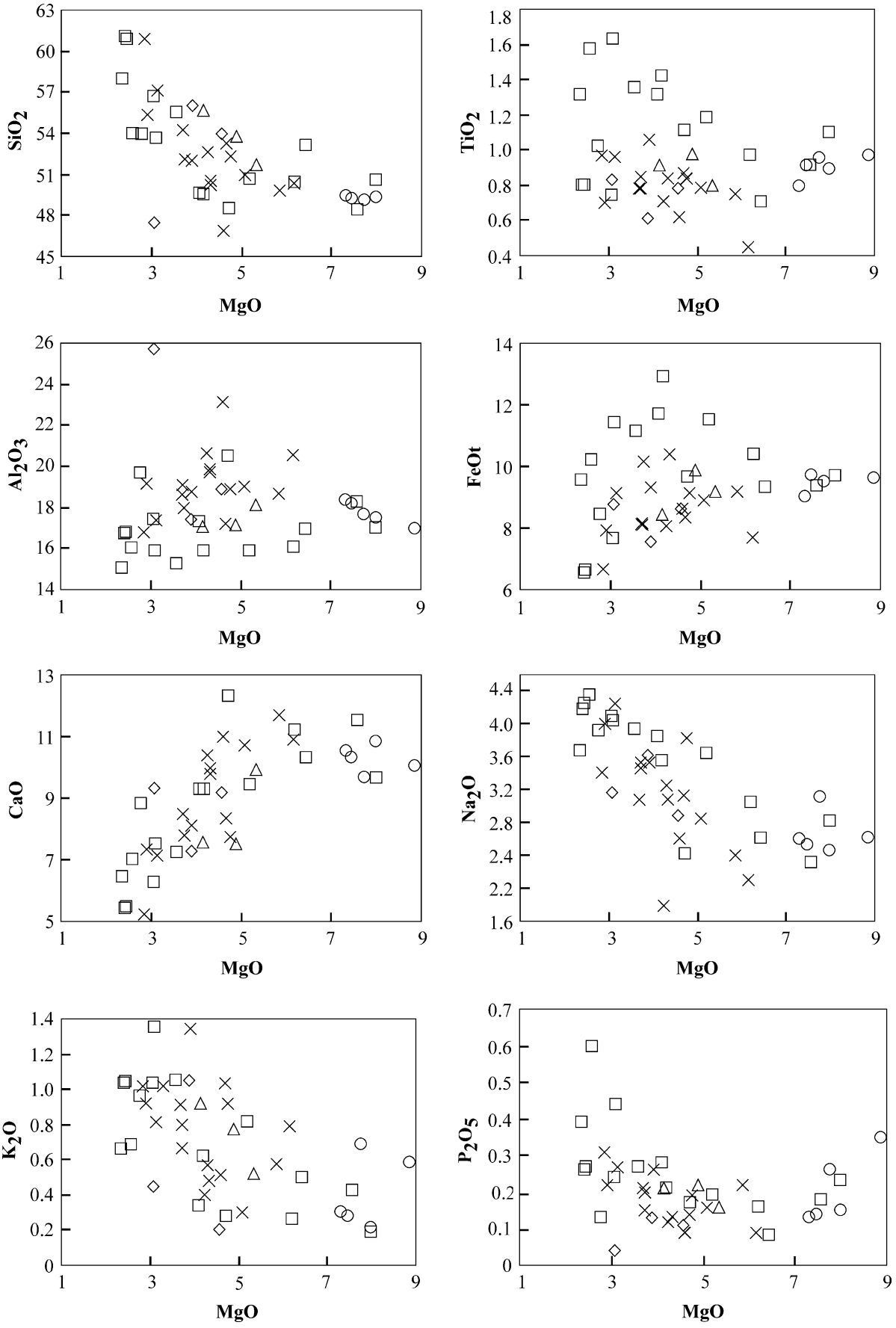


Fig. 4. Variation diagrams of major elements with respect to MgO. Symbols as in Fig. 3.

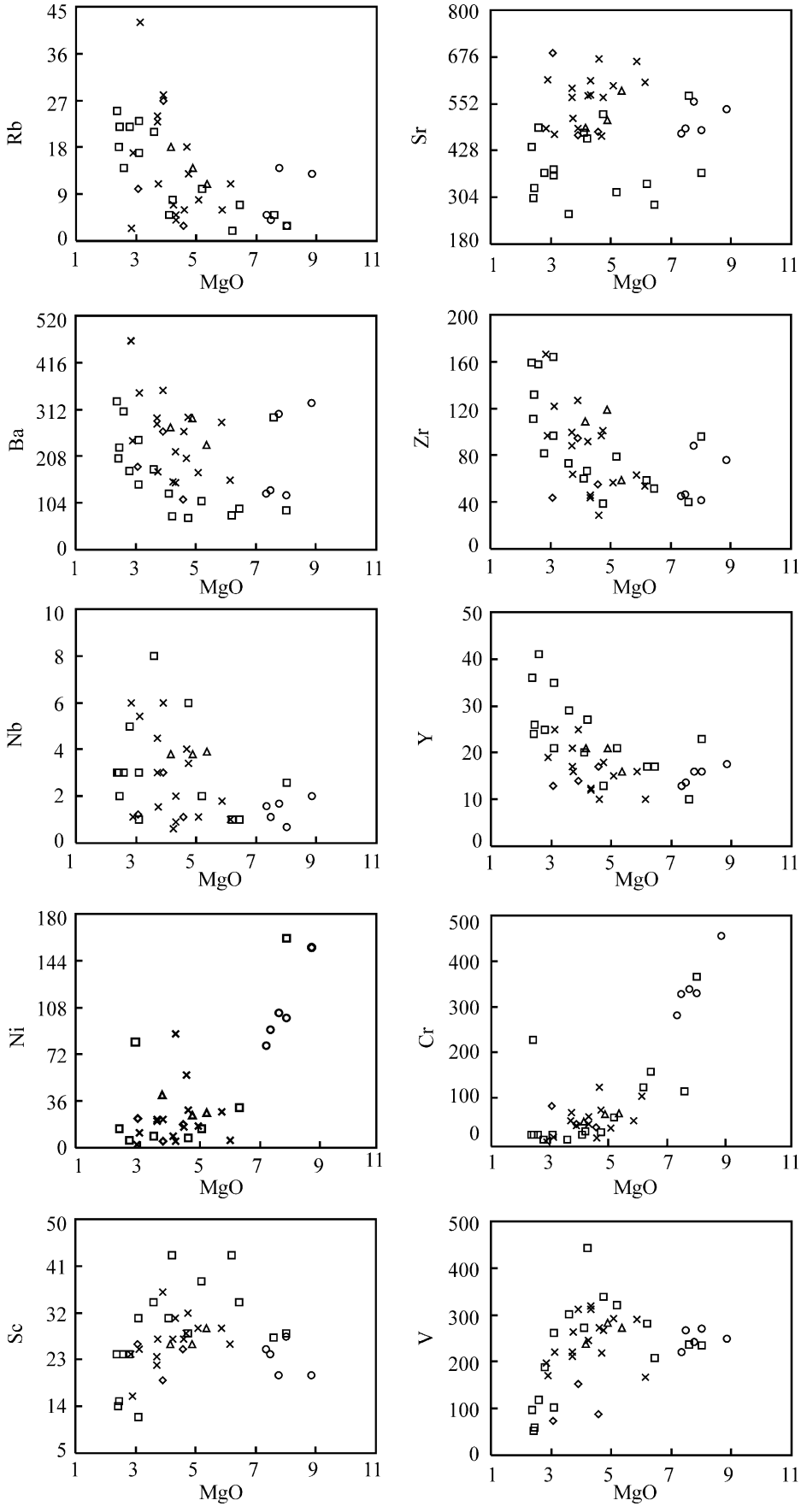


Fig. 5. Variation diagrams for selected trace elements with respect to MgO. Symbols as in Fig. 3.

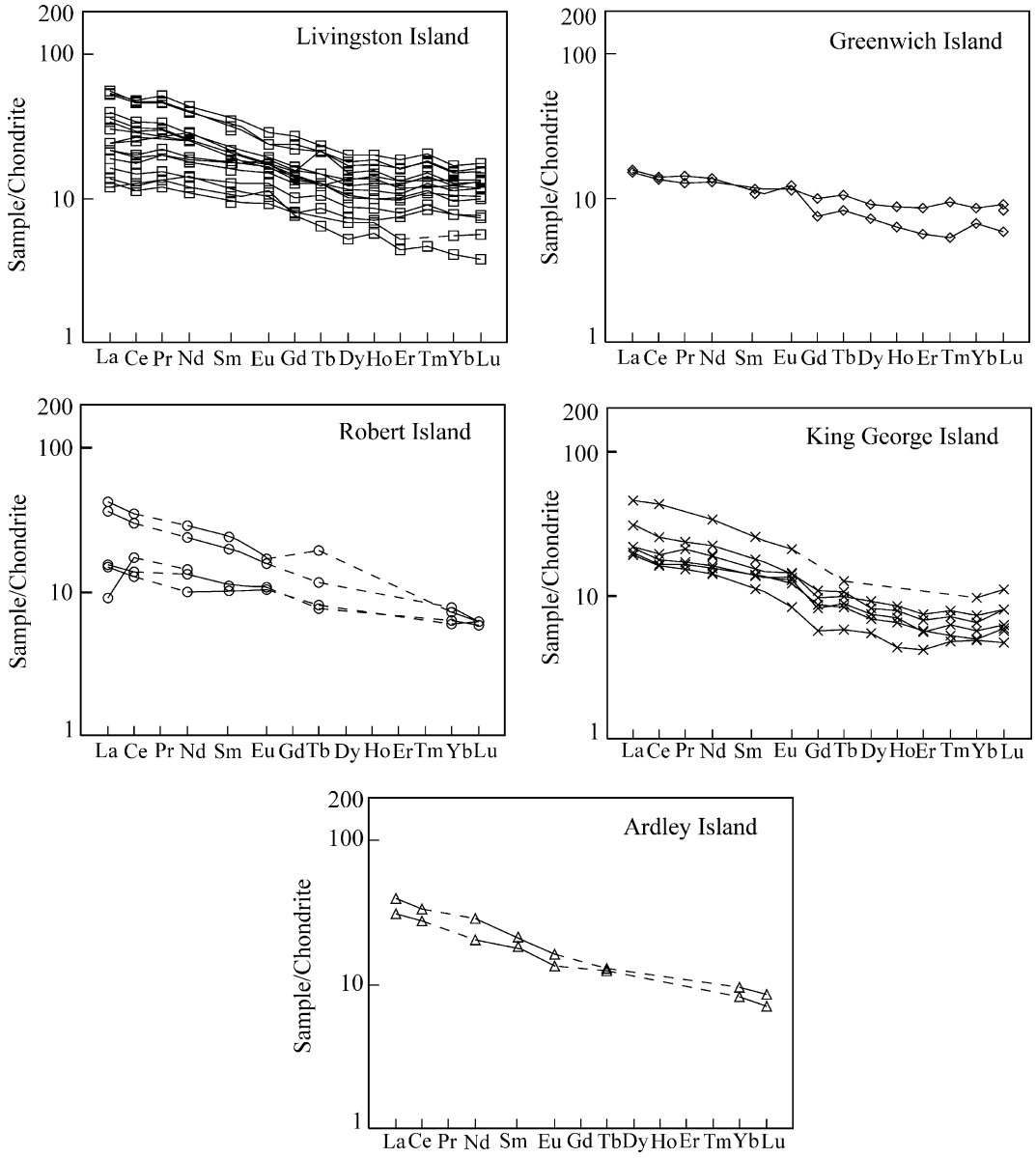


Fig. 6. Chondrite-normalized (Nakamura, 1974) REE patterns for selected samples. Dashed lines represent chemical elements not determined.

$(Ce/Yb)_N$ ratios vary around 5–20. The HREE patterns are relatively flat for all samples, with $(Gd/Lu)_N$ ratios greater than 3. The most primitive samples have $Yb_N < 10$, which indicates the presence of garnet as a residual phase in the mantle source.

Fig. 7 shows N-MORB-normalized trace element abundances in the South Shetland samples. All samples show a prominent Nb trough, characteristic of subduction zone magmas. This depletion of Nb relative to the large-ion lithophile elements (LILE; e.g., Rb, Ba, K) can be attributed primarily to two processes: (1) the addition of an LILE-enriched, Nb-poor fluid component to the mantle wedge or (2) the preferential retention of Nb in amphibole relative to other phases in the mantle source (Borg et al., 1997). Similar processes are inferred for the general depletion of the high field strength elements (HFSE)—Zr, Ti, and Y—with respect to the LILE in arc magmas (Pearce and Peate, 1995).

All South Shetland samples are enriched in Rb, Ba, K, and Sr relative to N-MORB, but they are depleted in Nb, Zr, Hf, and Ti. All samples show positive Ba and Sr anomalies. Weak negative Ti anomalies also are evident. Some samples from Livingston Island present high Y contents (41 ppm versus 27 ppm) compared with other samples that have similar MgO contents.

The South Shetland samples have moderate LREE enrichment relative to HREE, depletion in Nb relative to Yb with respect to N-MORB, and high Th/Yb ratios relative to N-MORB and ocean island basalts (OIB) (Fig. 8). These patterns suggest that the studied rocks are derived from magmas that originated from the partial melting of

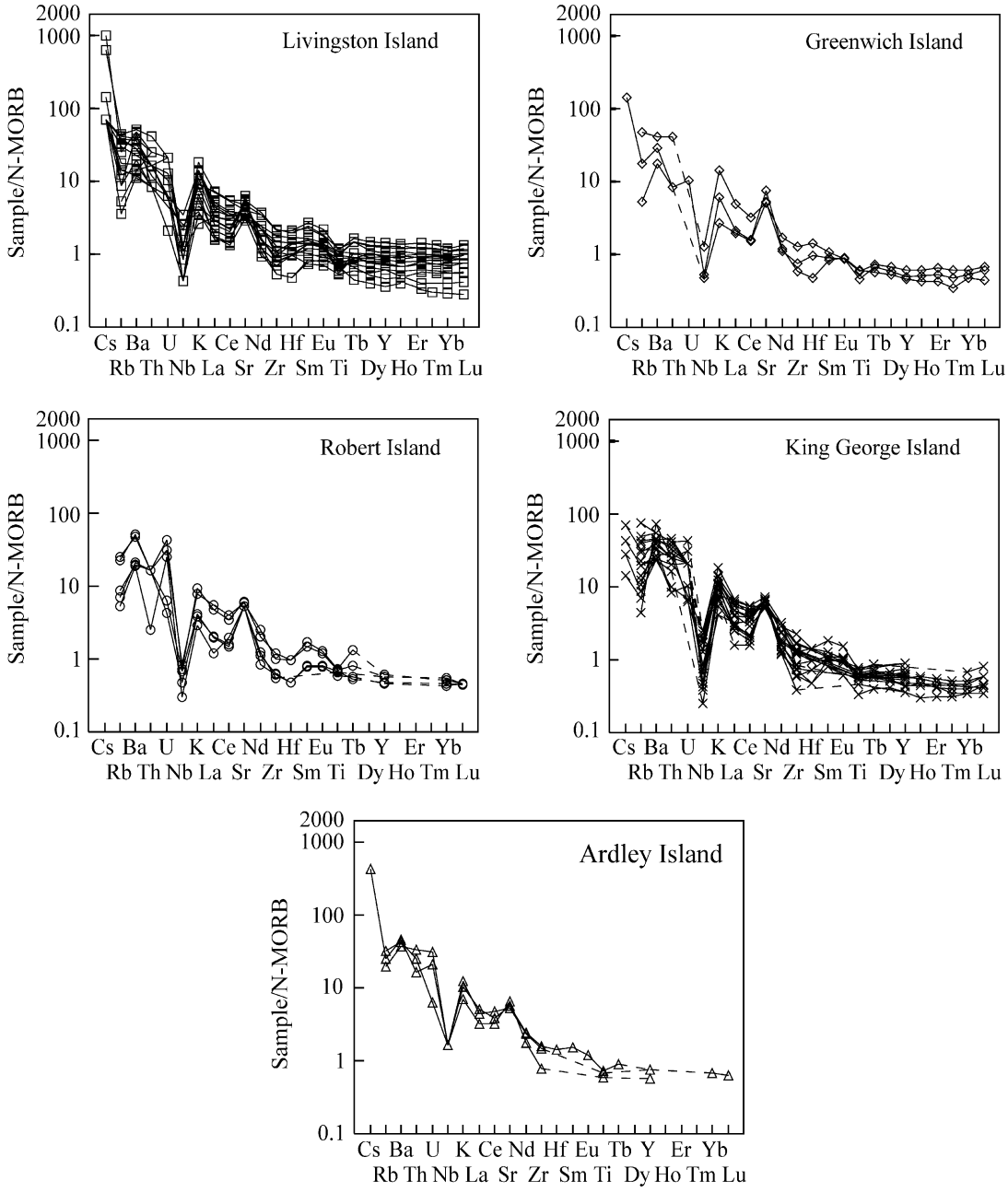


Fig. 7. N-MORB-normalized (Sun and McDonough, 1989) trace element diagrams. Dashed lines represent chemical elements not determined.

the lithospheric mantle, which was modified by fluids and sediments from a subduction zone.

The South Shetland samples plot in the AFM diagram at the limit between tholeiitic and calc-alkaline fields (Fig. 9 (a)). In the alkali index versus $Al_2O_3$ diagram (Fig. 9 (b)), most samples from King George Island and some from Livingston Island plot in the calc-alkaline field. The calc-alkaline affinity is confirmed by the LILE enrichment and low Nb, Zr, and $TiO_2$ contents. Mineral chemistry data also are compatible with the calc-alkaline series (Ewart, 1982; Machado et al., 2001).

Gradual LREE enrichment relative to HREE is observed in the youngest islands (King George and Ardley). Some samples from Livingston Island show an almost flat pattern, whereas samples from Greenwich Island show a moderate LREE enrichment. This trend continues in samples from Robert Island, but in the samples from King George and Ardley Islands, the REE pattern indicates an increase in the LREE enrichment relative to HREE.

The geochemistry patterns of the South Shetland Islands suggest gradual modifications in the source by subduction components. These modifications were responsible for

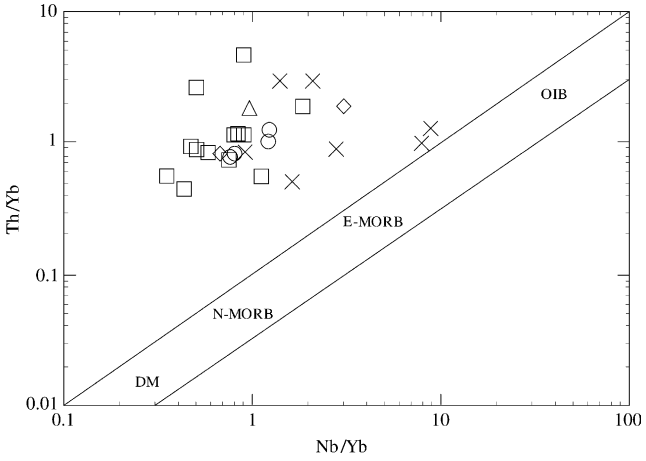


Fig. 8. Th/Yb versus Nb/Yb ratio (modified after Pearce and Peate, 1995). Th is often metasomatically added to arc mantle source regions, which leads to negative Nb anomalies characteristic of arc magmas. Here, rocks with very little subducted slab influence (non-arc) lie within the mantle array defined by the DM-N-MORB-E-MORB-OIB array. Samples with arc parentage or those influenced by subducted slab flux (BABB) lie on a different trajectory with higher Th at a given Nb content than do non-arc rocks. Symbols as in Fig. 3.

the evolution from tholeiitic to calc-alkaline patterns. This hypothesis presents a way to explain both the concentration of samples in tholeiitic and calc-alkaline fields on the AFM diagram and the REE patterns.

## 7. Discussion

The correlation of MgO with major and trace elements indicates that the South Shetland samples represent mantle melts that have experienced compositional modifications through fractional crystallization after segregation from their source regions. Phenocrysts of olivine, clinopyroxene, plagioclase, and Ti-magnetite occur in the samples, and fractionation of these minerals may explain the chemical variations. Olivine fractionation is implicit according to the positive correlation between Ni and MgO. The Sc and V contents decrease with decreasing MgO concentration, which suggests clinopyroxene's control, as supported by the correlation of the $CaO/Na_2O$ ratios with MgO content (Fig. 10). The $CaO/Na_2O$ ratio is virtually independent of melting pressure (Herzberg and Zhang, 1996) and olivine fractionation but very sensitive to clinopyroxene fractionation.

N-MORB-normalized patterns show that the studied samples, with the exception of LILE, are as impoverished in incompatible elements as is N-MORB. This impoverishment suggests that the South Shetland volcanic rocks were derived from a source similar to a depleted mantle but enriched in LILE (Fig. 7). The LILE enrichment can be explained by metasomatic modification of the depleted mantle source by subduction-derived fluids. In contrast to the LILE, the HFSE—such as Zr, Hf, Ti, and Nb—are relatively insoluble in aqueous fluids (Keppler, 1996).

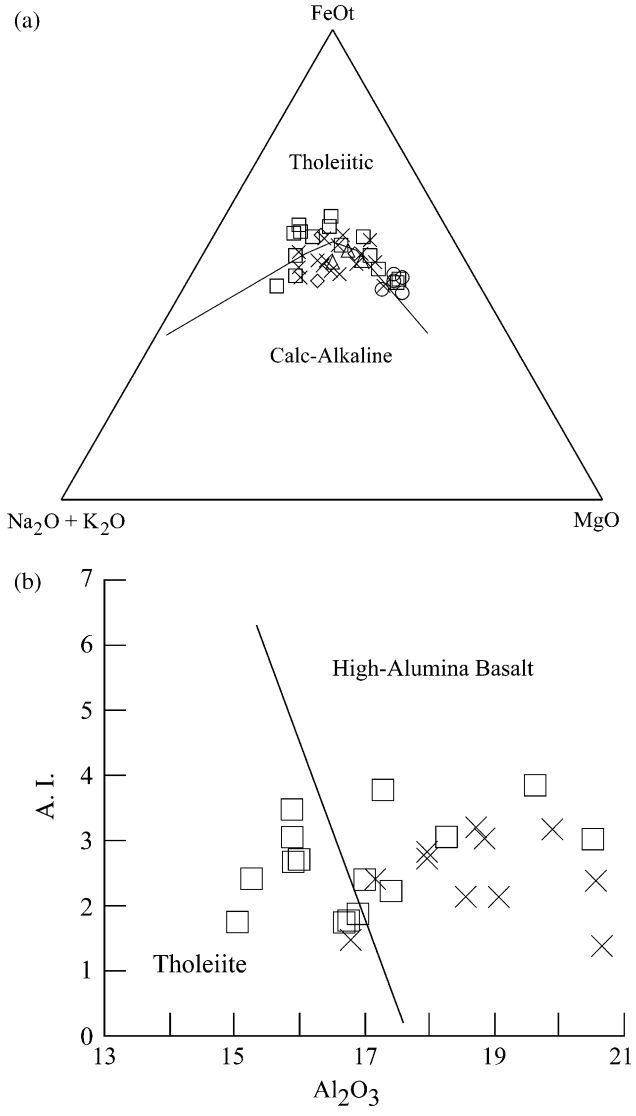


Fig. 9. AFM diagram showing South Shetland sample distribution (calc-alkaline and tholeiitic fields from Irvine and Baragar, 1971). Symbols as in Fig. 3.

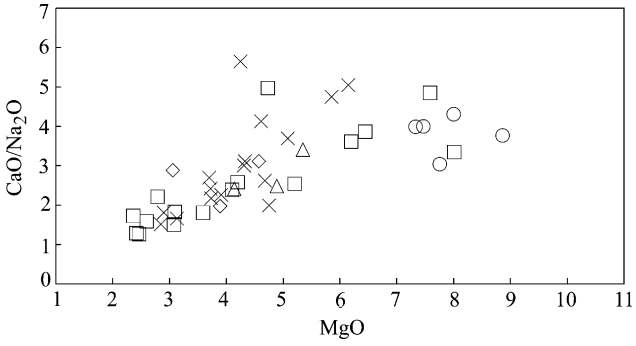


Fig. 10. $CaO/Na_2O$ ratio versus MgO diagram, suggesting significant clinopyroxene fractionation. Symbols as in Fig. 3.

In island arcs, therefore, these elements are derived predominantly from the mantle wedge, and their relative concentrations reflect the composition of the mantle wedge beneath the arc.

The South Shetland archipelago samples show a geochemical pattern that evolves from tholeiitic to calc-alkaline. Tholeiitic affinity is preserved in the samples from Livingston Island, which provides the oldest rocks. Calc-alkaline affinity is confirmed by the LILE enrichment and low Nb, Zr, and $TiO_2$ contents.

A model for magma genesis beneath the South Shetland Islands can be proposed on the basis of the prominent geochemical features of the erupted samples. This model is only one of several possible, but it is broadly consistent with the South Shetland data. According to this model, mantle upwelling and pressure-release melting occurs beneath the South Shetland Islands. In a geodynamic setting dominated by extensional tectonics for this part of Antarctic (Luft et al., 2002), the crust may be locally relatively thin, and thus, high melt fractions can be achieved through the melting of the hot, upwelling mantle. This process produces primary high-aluminum basaltic (HAB) magmas with low $SiO_2$ (if the melting begins at high pressures) and $Na_2O$ and high CaO, FeO, and $Al_2O_3$ that fractionate olivine, clinopyroxene, and calcic plagioclase during ascent to produce low-Mg HAB. After reaching the base of the crust, small batches of this magma exploit any extensional fractures and penetrate to the surface to erupt as cones. The rest may pond and fractionate further or intrude into the crust and supply a small crustal magma chamber beneath the main volcanic edifice. As fractionation proceeds, the residual liquid becomes increasingly volatile rich until saturation is reached and volatile exsolution takes place. Continuing exsolution increases the chamber pressure until eruption occurs. Crustal faults and fractures that intersect the chamber, possibly at deeper levels, act as conduits for flank cinder cones and perhaps fissure-style eruptions. The cones and flows are assumed to represent an earlier phase of volcanism.

## 8. Conclusion

The studied volcanic rocks represent magmas erupted in the South Shetland arc (Antarctica) between Mesozoic and Cenozoic times (143–44 Ma). Geochemical data obtained from the samples of the South Shetland archipelago suggest that magmatism evolved from a tholeiitic to a calc-alkaline series; some samples present transitional patterns. The available geochronological data show that rocks from Livingston Island present tholeiitic characteristics. The transition from a tholeiitic to a calc-alkaline pattern could be explained by fluids and sediments that were added to the mantle source during subduction.

Geochemical data indicate that the studied samples crystallized from evolved magma. The evolution of the South Shetland magmas was dominated by fractional crystallization of olivine, clinopyroxene, calcic plagioclase, Ti-magnetite, and minor orthopyroxene, which produced different magmatic liquids. The magmas show moderate to elevated $Al_2O_3$ (15–26 wt%) and variable MgO (2–9 wt%) contents. Ni and Cr values are low in most samples, which indicates that they do not represent primary depleted mantle magmas. High MgO, Cr, and Ni contents of samples from Robert Island may be related to olivine accumulation, a pattern also observed in two samples from Livingston Island. The $P_2O_5$ and Y patterns in the Robert and Livingston Island samples suggest apatite participation in the cumulatic assemblage.

The South Shetland archipelago magmatism involved lithospheric mantle melting modified by subduction components that generated basic liquids originally enriched in LILE relative to HFSE and LREE relative to HREE, depleted in Nb and Zr relative to Yb, and with a high Th/Yb ratio relative to N-MORB and OIB.

## Acknowledgements

John Stanley (University of Adelaide, Australia) is acknowledged for analytical support during data collection. Francisco Hervé Allamand (University of Chile) and Tania Dutra (UNISINOS) provided geological support and prompt donation of some Antarctic samples. Lauro Valentin Stoll Nardi (Federal University of Rio Grande do Sul) improved the text and provided useful comments. This research was supported by the Brazilian Antarctic Program (PROANTAR-CNPq), CAPES (Sandwich Program), PRONEX/IG-UFRGS, CNPq, the Antarctic Chilean Institute (INACH)/-Projects 01-95, 03-96, and the Antarctic Institutional Program of the University of Chile.

## References

Arculus, R.J., 1994. Aspects of magma genesis in arcs. Lithos 33, 189–208.

Azevedo, G.C., 1992. Caracterização geológica, geoquímica e geocronológica da Ilha Dee e parte da Ilha Greenwich, Arquipélago das Shetland do Sul, Antártica. M.Sc. Thesis. Federal University of Rio Grande do Sul, 184p.

Barker, P.F., Griffiths, D.H., 1972. The evolution of the Scotia Ridge and Scotia Sea. Philosophical Transactions of the Royal Society of London 271, 151–183.

Birkenmajer, K., Delitala, M.C., Narebski, W., Nicoletti, M., Petrucciani, C., 1986. Geochronology of Tertiary island-arc volcanics and glaciogenic deposits, King George Island, South Shetland Islands (West Antarctica). Bulletin of the Polish Academy of Earth Sciences 34 (3), 257–273.

Borg, L.E., Clynne, M.A., Bullen, T.D., 1997. The variable role of slab-derived fluids in the generation of a suite of primitive calc-alkaline lavas from the Southernmost Cascades, California. Canadian Mineralogist 35, 425–452.

Crame, J.A., Pirrie, D., Crampton, J.S., Duane, A.M., 1993. Stratigraphy and regional significance of the Upper Jurassic–Lower Cretaceous Byers Group, Livingston Island, Antarctica. Journal of the Geological Society of London 150, 1075–1087.

Ellam, R.M., Hawkesworth, C.J., 1988. Elemental and isotopic variations in subduction related basalts: evidence for a three component model. Contributions Mineralogy and Petrology 98, 72–80.

Ewart, A., 1982. The mineralogy and petrology of Tertiary—recent orogenic volcanic rocks with special reference to the andesite-basalt composicional range, in: Thorpe, R.S. (Ed.), Andesites: Orogenic Andesites and Related Rocks. Wiley, New York, pp. 25–95.

Figueiredo, A.M.G., Marques, L.S., 1989. Determination of rare earths and other trace elements in the Brazilian Geological Standards BB-1 and GB-1 neutron activation analysis. Geochimica Brasiliensis 3, 1–8.

Gill, J., 1981. Orogenic Andesites and Plate Tectonics. Springer, New York.

González-Ferrán, O., 1985. Volcanic and tectonic evolution of the northern Antarctic Peninsula—Late Cenozoic to Recent. Tectonophysics 114, 389–409.

Gracanin, T.M., 1983. Geochemistry and geochronology of some Mesozoic igneous rocks from the northern Antarctic Peninsula region. M.Sc. Thesis, Ohio State University.

Grikurov, G.E., Krylov, A., Polyakov, M.M., Covbun, N., 1970. Vozrast gornych porod v severnoj casti Antarkticeskogo Poluostrova i na Juznych Setlandskich ostrovach (po dannyum kalij-argonovogo metoda). Informationnyy Byulleten Sovetskoy Antarkticheskoy Ekspeditsii 80, 30–33.

Hamilton, W.B., 1995. Subduction systems and magmatism, in: Smellie, J.L. (Ed.), Volcanism Associated with Extension at Consuming Plate Margins Geological Society of London, Special Publication 81, pp. 3–28.

Hathway, B., 1997. Nonmarine sedimentation in an Early Cretaceous extensional continental-margin arc, Byers Peninsula. Livingston Island, South Shetland Islands. Journal of Sedimentary Research 67, 686–697.

Hathway, B., Lomas, S.A., 1998. The Upper Jurassic–Lower Cretaceous Byers Peninsula Group, South Shetland Islands, Antarctica: revised stratigraphy and regional correlations. Cretaceous Research 19, 43–67.

Herzberg, C., Zhang, J., 1996. Melting experiments on anhydrous peridotite KLB-1: Compositions of magmas in the upper mantle and transition zone. Journal of Geophysical Research 101, 8271–8295.

Hole, M.J., LeMasurier, W.E., 1994. Tectonic controls on the geochemical composition of Cenozoic mafic alkaline volcanic rocks from West Antarctica. Contributions Mineralogy and Petrology 117, 187–202.

Irvine, T.N., Baragar, R.A., 1971. A guide to the chemical classification of the common volcanic rocks. Canadian Journal of Earth Sciences 8, 523–548.

Keppler, H., 1996. Constraints from partitioning experiments on the composition of subduction-zone fluids. Nature 380, 237–240.

LeMaitre, R.W., 2002. Igneous Rocks: A Classification and Glossary of Terms. Cambridge University Press, Cambridge.

Luft Jr.., J.L., Machado, A., Chemale Jr.., F., 2002. Evidence of extensional tectonic in the northern Antarctic Peninsula, Antarctic. Journal of the South American Earth Sciences 2002;, 16.

Machado, A., 1997. Petrologia, geoquímica e geologia estrutural da Península Fildes. Ilha Rei George, Antártica. M.Sc. Thesis, Federal University of Rio Grande do Sul, 182p.

Machado, A., Lima, E.F., Chemale Jr.., F., Liz, J.D., Ávila, J.N., 2001. Química mineral das rochas vulcânicas da Península Fildes (Ilha Rei George), Antártica. Revista Brasileira de Geociências 31 (3), 291–298.

Moore, E.M., Twiss, R.J., 1995. Tectonics. W.H. Freeman and Company, New York.

Nakamura, N., 1974. Determination of REE, Ba, Fe, Mg, Na and K in carbonaceous and ordinary chondrites. Geochimica et Cosmochimmica Acta 38, 757–775.

Oteíza, O., 1999. Petrogénesis del magmatismo básico del Meso-Cenozoico en la Península Byers, Isla Livingston (Archipélago de Shetland del Sur, Antártica), University of Chile.

Pankhurst, R.J., Riley, T.R., Fanning, C.M., Kelley, S.P., 2000. Episodic silicic volcanism in Patagonia and the Antarctic Peninsula: chronology of magmatism associated with the break-up of Gondwana. Journal of Petrology 5 (41), 605–625.

Pankhurst, R.J., Weaver, S.D., Brook, M., Saunders, A.D., 1979. K–Ar chronology of Byers Peninsula, Livingston Island, South Islands. British Antarctic Survey Reports 49, 277–282.

Pearce, J.A., 1982. Trace element characteristics of lavas from destructive plate boundaries, in: Thorpe, R.S. (Ed.), Andesites: Orogenic Andesites and Related Rocks. Wiley, New York, pp. 525–548.

Pearce, J.A., Peate, D.W., 1995. Tectonic implications of the composition of volcanic arc magmas. Annual Review Earth and Planetary Science Letters 23, 251–285.

Peccerillo, A., Taylor, S.R., 1976. Geochemistry of Eocene calc-alkaline volcanic rocks from the Kastamonu area, northern Turkey. Contributions Mineralogy and Petrology 58, 63–81.

Smellie, J.L., Davies, R.E.S., Thomson, M.R.A., 1980. Geology of a Mesozoic intra-arc sequence on Byers Peninsula, Livingston Island, South Shetland Islands. British Antarctic Survey Reports 50, 55–76.

Smellie, J.L., Pankhurst, R.J., Thomson, M.R.A., Davies, R.E.S., 1984. The geology the South Shetland Islands: VI. Stratigraphy, geochemistry and evolution. British Antarctic Survey Reports, 87, 83p.

Sun, S.S., McDonough, W.F., 1989. Chemical and isotopic systematics of oceanic basalts: Implications for mantle composition and processes, in: Saunders, A.D., Norry, M.J. (Eds.), Magmatism in the Ocean Basins Geological Society of London, Special Publication 42, pp. 313–345.

Tatsumi, Y., Eggins, S., 1995. Subduction Zone Magmatism. Blackwell Science, Cambridge, MA.

Taylor, S.R., McLennan, S.M., 1985. The Continental Crust: Its Composition and Evolution. Blackwell, Oxford.

Vukadinovic, D., 1993. Are Sr enrichments in arc basalts due to plagioclase accumulation? Geology 21, 611–614.